JACS
JOURNAL OF THE AMERICAN CHEMICAL SOCIETY
Communication
pubs.acs.org/JACS

An Unconventional Role of Ligand in Continuously Tuning of Metal–Metal Interfacial Strain

Yuhua Feng,[†] Jiating He,[†] Hong Wang,[†] Yee Yan Tay,[‡] Hang Sun,[†] Liangfang Zhu,[†] and Hongyu Chen*[,†]

[†]Division of Chemistry and Biological Chemistry, Nanyang Technological University, Singapore 637371
[‡]School of Materials Science and Engineering, Nanyang Technological University, Singapore 639798

Supporting Information

ABSTRACT: We show that embedding of a surface ligand can dramatically affect the metal–metal interfacial energy, making it possible to create nanostructures in defiance of traditional wisdom. Despite matching Au–Ag lattices, Au–Ag hybrid NPs can be continuously tuned from concentric core–shell, eccentric core–shell, acorn, to dimer structures. This method can be extended to tune even Au–Au and Ag–Ag interfaces.

Fabricating nanomaterials with structural order is a critical step toward complex objects and ultimately functional nanodevices.[1] Going beyond single-component nanoparticles (NPs), hybrid NPs[1c,d] have yet to be fully explored. Integration of multiple components offers not only combined physical properties but sometimes new or enhanced properties due to the coupling effects.[2] In doing so, the single most important factor is the interfacial energy between the components, which governs the growth process. The knowledge in and the ability to tune this energy[3] are essential for rational design and synthesis.

It is generally difficult to assemble prefabricated NPs with precise order.[4] Typically, hybrid NPs were synthesized by depositing a growth material (GM) on seed NPs.[5] It is generally accepted that the lattice match between GM and seed is the dominant factor in determining the growth mode: When the lattice mismatch is small, GM can epitaxially overgrow on the seed surface (the Frank–van der Merwe, or FM growth mode),[6] leading to concentric core–shell structure. Typical examples include Au@Ag and Pt@Pd NPs.[5a,b] When the mismatch is large, GM often forms segregated islands on the seed NPs to reduce the interface in between (the Volmer–Weber, or VW growth mode).[5c,6] That is, once GM forms nuclei on the seed, it is more favorable to deposit on these sites than on ligand-coated seed surface. Growth of metal on oxide or on semiconductor often follows this mode.[5d,e] In an intermediate mode, GM first forms a thin concentric shell, which is strained due to moderate lattice mismatch. When this wetting layer reaches a critical thickness, the accumulated strain becomes large enough so that the subsequent growth forms "coherent" islands (the Stranski–Krastanov, or SK growth mode).[6] An important consequence of the above conventional wisdom is that once GM and seed are chosen, the lattice (mis)match and growth mode are set.

Unusual hybrid NPs have been reported. Despite matching Au–Ag lattices, Au–Ag heterodimers were synthesized when the seed AuNPs were confined at the interface of Pickering emulsion.[7a] Ouyang's group showed that core–shell NPs can undergo exchange reaction and gave rise to two substantially lattice-mismatched components while maintaining core–shell structure.[7b] Recently, Xia and co-workers showed that Au/Ag growth on Pd seeds can form either concentric core–shell or heterodimer structure by choosing different reductants for Au, or by manipulating the kinetics of Ag reduction.[8]

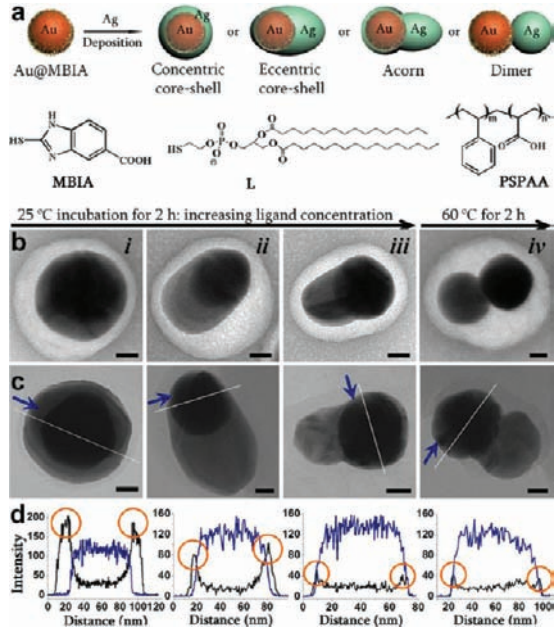

Figure 1. (a) Schematics illustrating the Au–Ag hybrid NPs and diagrams of relevant molecules; (b) TEM images of sample ***i–iv*** with stained background; and (c, d) HRTEM and corresponding EDS line scan showing the presence of Ag (black line) on the Au (blue) surface. Scale bars: 20 nm.

The importance of ligands in growing metal nanocrystal is well-known, but their traditional roles are limited on the surface of facets. During metal deposition, the ligands dynamically adsorb and desorb on the seed surface, affecting the growth of underlying facets. Facets with preferred ligand binding are less exposed and thus grow slower.[9] Herein, we demonstrate that by simply varying ligand conditions during the growth of Ag on Au

Received: November 25, 2011
Published: January 10, 2012

dx.doi.org/10.1021/ja211086y | J. Am. Chem.Soc. 2012, 134, 2004–2007

seeds, the morphology of Au−Ag hybrid NPs can be *continuously* tuned (Figure 1). The variability in the growth mode contradicts conventional wisdom, probably because the embedded ligand becomes a dominant factor for the metal−metal interfacial energy and thus dictates the growth mode of Ag. This knowledge in tuning the interface between two components will inspire new synthetic designs.

We treated citrate-stabilized AuNPs with 2-mercaptobenzoimidazole-5-carboxylic acid (MBIA) and used them as seeds for growing Ag. The names of the resulting hybrid NPs (vide infra) are defined according to Figure 1a; their main difference is the contact area of the Ag island. In a typical synthesis, 1 mL of as-synthesized AuNPs (d = 50 nm, 157 pM in *number* of NPs)[10] were incubated with MBIA, whose concentration was varied from 1, 5, to 20 μM (designated as samples ***i***, ***ii***, and ***iii***, respectively). After 2 h incubation at room temperature, reductant hydroquinone (HQ, 0.5 mM) was added to this solution, followed by dropwise addition of $AgNO_3$ (0.5 mM) to initiate their reaction. An additional sample ***iv*** was generated by incubating AuNPs with 20 μM MBIA at 60 °C to enhance ligand coordination; the solution was cooled to room temperature before Ag growth. The final color of the hybrid NPs appeared orange to brown under reflected light (Figure 2).

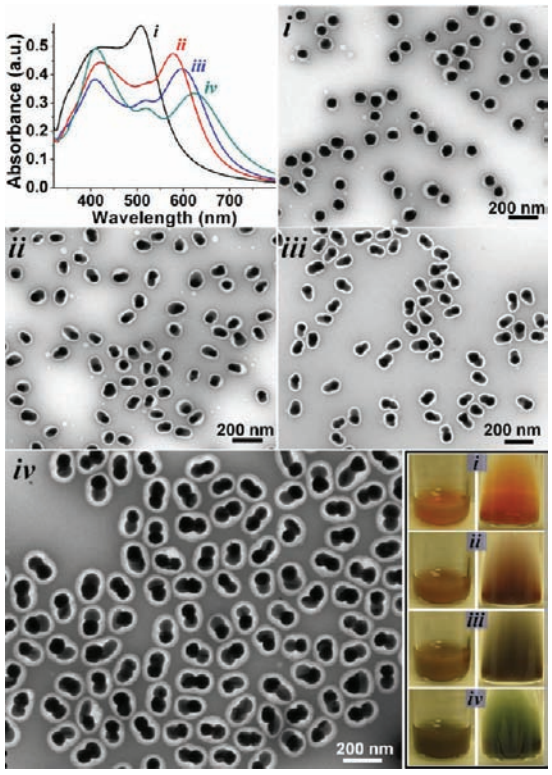

Figure 2. UV−vis extinction spectra and TEM images of samples ***i***−***iv***. The hybrid NPs were prepared by incubating Au seeds with (***i***) 1, (***ii***) 5, or (***iii***) 20 μM MBIA at room temperature for 2 h, or with (***iv***) 20 μM MBIA at 60 °C for 2 h. The photographs show the samples under reflected (left) and transmitted (right) light.

However, under transmitted light the samples appeared quite different, particularly the sample ***iv*** containing heterodimer NPs. Most likely, strong absorption and scattering of red light made it unable to pass through the sample, but this portion of red light was included in the reflected light. In UV−vis extinction spectra, the samples containing eccentric core−shell, acorn, and dimer NPs showed three bands: Ag transverse plasmon absorption at around 400 nm, weak Au transverse absorption at around 520 nm, and Au−Ag longitudinal absorption that ranged from 570 to 630 nm (Figure 2). Obviously, the third band was affected by the different Ag islands. The sample ***i*** containing concentric NPs only showed two bands at 400 and 520 nm without longitudinal plasmon absorption.

To prevent the hybrid NPs from aggregating, they were encapsulated in shells of polystyrene-*block*-poly(acrylic acid) (PSPAA),[11] before being characterized by transmission electron microscopy (TEM). As previously reported,[4a,11] we used a thiol-ended hydrophobic ligand, 1,2-dipalmitoyl-*sn*-glycero-3-phosphothioethanol (**L**), to render the NP hydrophobic for the adsorption of PSPAA. After the encapsulation, the UV−vis spectra of the samples did not show obvious changes except slight red-shift of the absorption bands[10] due to increase of the refractive index of the medium surrounding the NPs.[11a]

The PSPAA shells are difficult to see in Figure 1c, but they are very obvious against a negatively stained background. The Ag domains always show lower contrast in TEM than those of Au. As shown in Figure 2, all four types of the hybrid NPs are uniform in size and shape;[10] their structures were also presented as enlarged TEM images in Figure 1b,c. Only at the low [MBIA] of 1 μM was concentric Au@Ag core−shell structure obtained. In samples ***ii*** and ***iii***, the increasing [MBIA] caused the Ag domain to increasingly shift to one side in the hybrid NPs, forming a single island. However, even on the Au surface away from the Ag island there was always a thin Ag layer, which was verified by energy-dispersive X-ray spectroscopy (EDS) line scan (Figure 1d). The formation of such a thin layer of GM is typical of the SK growth mode.[6] In sample ***iv*** where the seeds were incubated with 20 μM MBIA at elevated temperature, the grown Ag domains were quite segregated from the Au seed, so that the hybrid NPs almost appeared as two juxtaposed prefabricated NPs. The purity of such heterodimers reached 98.3% (out of 529 NPs surveyed). The overcoating Ag layer was barely detectable, and thus, the growth started to resemble the VW mode.

It is surprising that the growth mode of Ag can be continuously varied by changing only the ligand conditions. Longer incubation time or higher incubation temperature lead to denser surface ligands.[9] To understand whether the seeds or the newly generated Ag surface were being affected, experiments were carried out with exactly the same ligand concentration, but different incubation conditions. Comparing samples ***iii*** and ***iv***, the 60 °C incubation led to significantly smaller contact area of the Ag island than that resulted from room temperature incubation. When the incubation step was removed, that is, the Au seeds were treated with 20 μM MBIA immediately before Ag reduction, only concentric core−shell NPs were obtained (Figure 3a). The importance of the incubation step suggests that the critical factor was the ligand density on the initial Au seeds. However, such a conclusion contradicts the traditional belief that ligands have to leave, often dynamically, before metal can deposit on the underlying facets. During Ag growth, if the surface-bound MBIA have to eventually leave, then the initial ligand density should not have made such a difference.

There is a possibility that the different incubation conditions may introduce unexpected chemical species or lead to different rate of Ag reduction. Thus, we tried to reproduce different growth conditions in a single solution, so that *all* chemical

dx.doi.org/10.1021/ja211086y | *J. Am. Chem.Soc.* 2012, 134, 2004−2007

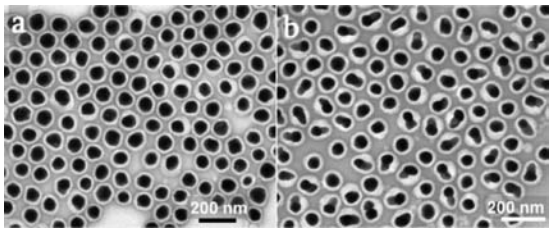

Figure 3. Control experiments showing that (a) concentric core−shell NPs were obtained when Au seeds were directly treated with 20 μM MBIA without incubation and (b) a mixture of concentric core−shell and acorn NPs was obtained when fresh seeds were mixed with seeds preincubated with 20 μM MBIA at 60 °C.

species and the rate of Ag reduction are exactly identical: We added 1 equiv of citrate-stabilized AuNPs to a sample that had undergone 60 °C incubation with 20 μM MBIA. After Ag growth and PSPAA encapsulation, the resulting NPs showed roughly 1:1 mixture of concentric core−shell and dimeric NPs (Figure 3b). The divergence of growth modes here argues against any significant role of ligands during the Ag reduction.

It is well-known that Ag and Au have small lattice mismatch (<0.2%). In most literature reports, Ag formed a "wetting" conformal layer on Au surfaces. Typically, one would expect that if the ligands cannot dissociate, the GM would simply homogeneously nucleate in the solution without attaching to the seeds. The ligand MBIA has clearly altered the surface of the Au seeds but somehow still allow Ag deposition. Considering the unusual tunability of growth modes, we have to hypothesize that some of the MBIA molecules were embedded at the Au−Ag interface and thus affect the interfacial energy.

Previously, we reported that embedding of Raman-active molecules such as 4-mercaptobenzoic acid (MBA) or 4-aminothiophenol (ATP) inside a metal layer could gave rise to greatly enhanced signals of surface-enhanced Raman scattering (SERS).[12] The incubation step of Au seeds with ligand prior to Ag growth was found to be important for generating strong SERS signals. This observation, along with others, suggested that the ligands were likely embedded in metal layers. Enhanced SERS signal was also observed when MBIA was used as the ligand, but the anisotropic growth of Ag complicated the SERS interpretation. Detailed SERS studies will be reported in a separate article; we only focus on nanocrystal growth here.

If MBIA molecules are embedded at the Au−Ag interface, a natural question is whether molecules on the freshly generated Ag surface can be similarly embedded. To answer this question, we prepared a fresh batch of sample ***iv***; after synthesis the solution was incubated at room temperature for 2 h before the addition of HQ and $AgNO_3$ to achieve a second cycle of Ag growth (MBIA was in excess and not replenished). The NPs were then encapsulated in PSPAA, purified, and characterized. As shown in Figure 4a, trimeric hybrid NPs were obtained with excellent purity (97.3% out of 923 particles surveyed).[10] Probably MBIA cannot securely anchor/pack on a freshly generated Ag surface during Ag growth. This scenario is similar to that in Figure 3a, where the ligand incubation step was removed. After the "new" Ag surface was covered with MBIA in an additional incubation step; the strong binding of ligands, likely assisted with regional packing order, forced the subsequent Ag growth into islands. Since there is no lattice mismatch at Ag−Ag interface, the strain must come from

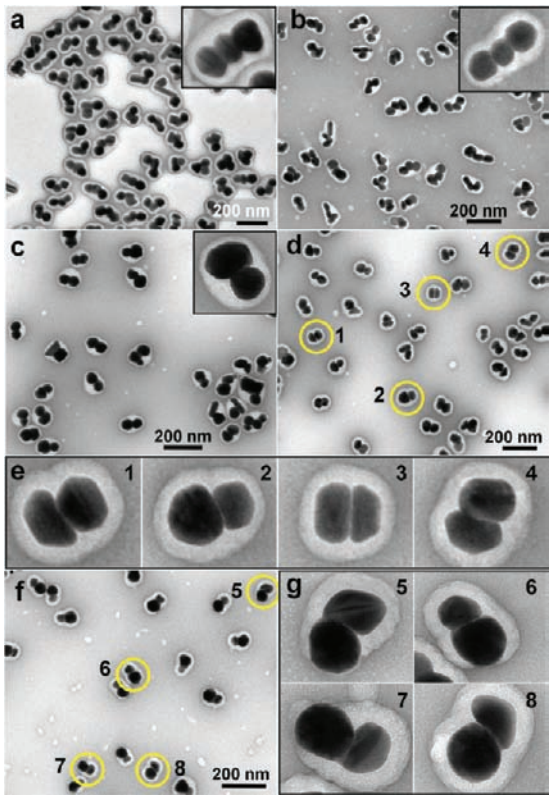

Figure 4. TEM images of (a) Au−Ag−Ag; and (b) Ag−Ag−Ag trimers prepared by the second cycle of Ag grown on the Au−Ag and Ag−Ag dimers, respectively; (c) Au−Au and (d) Ag−Ag dimers; (f) Au−Ag heterodimers prepared by incubating seeds with 150 μM MBIA at 60 °C for 2 h; (e, g) enlarged images selected from d and f.

embedded ligands. Remarkably, the new Ag island always occurred on the Ag domain of the starting Au−Ag dimer. This is surprising because the Au domain is covered with a thin Ag layer. Repeating Ag growth on sample ***iii*** (room temperature incubation with 20 μM MBIA in both cycles) also did not form a second Ag island on the Au seeds.[10] A likely reason is that the thin Ag layer is strained as in the SK growth mode.

With this discovery, it is not surprising that Au−Au and Ag−Ag dimers can be generated using the same method. Figure 4c shows a sample of Au−Au dimers obtained by using citrate-stabilized AuNPs as seeds, ascorbic acid as reductant, and $HAuCl_4$ as Au precursor; Figure 4d shows a Ag−Ag dimer sample obtained by using Au@Ag NPs as a replacement for Ag seeds (15 nm AuNPs coated with a thick Ag shell, $d_{overall}$ = 45 nm); all other conditions were the same as sample ***iv***.[10] Similarly, Ag−Ag−Ag trimers were also obtained (Figure 4b).

In Figure 4d,e clear gaps of 1−2 nm in width can be observed in the Ag−Ag dimers. It appeared that when the embedded MBIA reached a certain density, the ligand layer can produce enough contrast to be observed by TEM. Thus, we incubated Au seeds with increased [MBIA] (150 μM) at 60 °C for 2 h. In the resulting Au−Ag hybrid NPs, a clear gap of 1−2 nm was also observed (Figure 4f,g). In comparison to sample ***iv***, the only difference was the ligand concentration used, and thus, we conclude that this gap contained embedded MBIA.

In depositing Ag, the exposed Au surface should be more favorable than the MBIA-covered Au surface. This argument is consistent with the formation of Ag island (as opposed to a concentric shell) at high ligand concentration. In other words,

dx.doi.org/10.1021/ja211086y | *J. Am. Chem.Soc.* 2012, 134, 2004−2007

the growth likely started from the "holes" of the MBIA layer. However, an important question is *did the Ag growth only occurred at the holes*. Since the Au seeds we used were polycrystalline with large size (50 nm), it is highly likely that multiple similar holes exist on each AuNP. Under the above hypothesis, we should have obtained multiple Ag islands with small contact area (as segregated islands) because they have to minimize the Au−ligand−Ag interface. In contrast, we obtained *coherent* Ag islands in samples ***ii*** and ***iii***. Most importantly, different surface ligand density would only lead to different sizes or numbers of the "holes", and thus, this hypothesis cannot explain the observed tunability of growth modes.

We believe that some MBIA molecules are embedded, even though most of them dynamically adsorb/desorb on the seeds. The probability of embedding is likely correlated with surface ligand density prior to Ag deposition, and this explains well the critical importance of the incubation step. The presence of such organic defects at the Au−Ag interface inevitably introduces strain in the metal lattices. As such, the Au−Ag interfacial energy is dramatically affected and causes the growth mode to change. In crystal growth, the thermodynamics and kinetics are well established in the FM, SK, and VW growth modes.[6] The sample ***ii*** with eccentric core−shell NPs can be viewed as an intermediate between FM and SK modes. As it is well-known in colloidal science, the relative strength of interfacial energies determines whether two materials form core−shell or dimer structures.[3a] Indeed, their morphology is *continuously* tunable between these two extremes. This principle can be applied to hybrid NPs, whose stabilities are determined by Au−solvent, Au−Ag, and Ag−solvent interfacial energies. Basically, the more unfavorable the Au−Ag interface, the more the Ag islands want to be segregated from the Au seeds to reduce their interface.

As we are finalizing this manuscript, we noted that an online publication reported the tuning of Pd−Ag hybrid NPs by varying the rate of Ag reduction.[8b] In our work, *only* the ligand concentration and incubation conditions were varied. Most importantly, the divergence of growth modes in a single solution (Figure 3b) and the formation of overcoating Ag layer in samples ***ii*** and ***iii*** rule out the effects of Ag deposition kinetics in this system. Moreover, the formation of clear gaps (Figure 4d−g) provides evidence for the embedded MBIA.

The size of our hybrid NPs can be readily tuned. Different sizes of seed NPs can be used, and by modifying the amount of HQ and Au/Ag precursors, the size of the GM domains can be easily modulated.[10] In combination with the controls in growth modes and multistep growth (e.g., to form trimers), our method is versatile in fabricating complex hybrid NPs.

In summary, we have demonstrated facile seeded growth of hybrid NPs with controllable morphology. The embedding of MBIA is probably a dominant factor in tuning the Au−Ag interfacial energy. The ligand MBIA is special in that it has a thiol group (that strongly anchors it on metal) and a diametric −COOH group (that is amenable for Au/Ag deposition). The fundamental understanding could be potentially exploited in other systems. The rational design and synthesis of complex nanostructure will provide the tool box for future endeavors in the fabrication of functional nanodevices.

■ ASSOCIATED CONTENT

Ⓢ Supporting Information

Details of experimental procedures, large-area view of TEM images. This material is available free of charge via the Internet at http://pubs.acs.org.

■ AUTHOR INFORMATION

Corresponding Author
hongyuchen@ntu.edu.sg

■ ACKNOWLEDGMENTS

We thank the MOE (ARC 13/09) and the A*Star (102-152-0018) of Singapore for financial support.

■ REFERENCES

(1) (a) Gao, J.; Gu, H.; Xu, B. *Acc. Chem. Res.* **2009**, *42*, 1097. (b) Wang, D.; Li, Y. *Adv. Mater.* **2011**, *23*, 1044. (c) Cortie, M. B.; McDonagh, A. M. *Chem. Rev.* **2011**, *111*, 3713. (d) Jones, M. R.; Osberg, K. D.; Macfarlane, R. J.; Langille, M. R.; Mirkin, C. A. *Chem. Rev.* **2011**, *111*, 3736. (e) Wang, F.; Han, Y.; Lim, C. S.; Lu, Y.; Wang, J.; Xu, J.; Chen, H.; Zhang, C.; Hong, M.; Liu, X. *Nature* **2010**, *463*, 1061. (f) Buck, M. R.; Bondi, J. F.; Schaak, R. E. *Nat. Chem.* **2012**, *4*, 37.

(2) (a) Costi, R.; Saunders, A. E.; Elmalem, E.; Salant, A.; Banin, U. *Nano Lett.* **2008**, *8*, 637. (b) Gu, H.; Zheng, R.; Zhang, X.; Xu, B. *J. Am. Chem. Soc.* **2004**, *126*, 5664. (c) Wang, F.; Li, C.; Sun, L. D.; Wu, H.; Ming, T.; Wang, J.; Yu, J. C.; Yan, C. H. *J. Am. Chem. Soc.* **2010**, *133*, 1106. (d) Yin, A. X.; Min, X. Q.; Zhang, Y. W.; Yan, C. H. *J. Am. Chem. Soc.* **2011**, *133*, 3816.

(3) (a) Torza, S.; Mason, S. G. *J. Colloid Interface Sci.* **1970**, *33*, 67. (b) Carbone, L.; Cozzoli, P. D. *Nano Today* **2010**, *5*, 449.

(4) (a) Wang, Y.; Chen, G.; Yang, M.; Silber, G.; Xing, S.; Tan, L. H.; Wang, F.; Feng, Y.; Liu, X.; Li, S.; Chen, H. *Nat. Commun.* **2010**, *1*, 87. (b) Chen, G.; Wang, Y.; Tan, L. H.; Yang, M. X.; Tan, L. S.; Chen, Y.; Chen, H. *J. Am. Chem. Soc.* **2009**, *131*, 4218. (c) Chen, G.; Wang, Y.; Yang, M. X.; Xu, J.; Goh, S. J.; Pan, M.; Chen, H. *J. Am. Chem. Soc.* **2010**, *132*, 3644.

(5) (a) Habas, S. E.; Lee, H.; Radmilovic, V.; Somorjai, G. A.; Yang, P. *Nat. Mater.* **2007**, *6*, 692. (b) Fan, F.; Liu, D.; Wu, Y.; Duan, S.; Xie, Z.; Jiang, Z.; Tian, Z. *J. Am. Chem. Soc.* **2008**, *130*, 6949. (c) Lim, S. I.; Varon, M.; Ojea-Jimenez, I.; Arbiol, J.; Puntes, V. *J. Mater. Chem.* **2011**, *21*, 11518. (d) Yang, J.; Peng, J.; Zhang, Q.; Peng, F.; Wang, H.; Yu, H. *Angew. Chem., Int. Ed.* **2009**, *48*, 3991. (e) Huang, S.; Huang, J.; Yang, J.; Peng, J. J.; Zhang, Q.; Peng, F.; Wang, H.; Yu, H. *Chem.—Eur. J.* **2010**, *16*, 5920.

(6) (a) Bauer, E. *Z. Kristallogr.* **1958**, *110*, 372. (b) Herman, M. A.; Richter, W.; Sitter, H. *Epitaxy: Physical Principles and Technical Implementation*; Springer: New York, 2004. (c) Peng, Z.; Yang, H. *Nano Today* **2009**, *4*, 143.

(7) (a) Gu, H.; Yang, Z.; Gao, J.; Chang, C. K.; Xu, B. *J. Am. Chem. Soc.* **2004**, *127*, 34. (b) Zhang, J.; Tang, Y.; Lee, K.; Ouyang, M. *Science* **2010**, *327*, 1634.

(8) (a) Lim, B.; Kobayashi, H.; Yu, T.; Wang, J.; Kim, M. J.; Li, Z. Y.; Rycenga, M.; Xia, Y. *J. Am. Chem. Soc.* **2010**, *132*, 2506. (b) Zeng, J.; Zhu, C.; Tao, J.; Jin, M.; Zhang, H.; Li, Z. Y.; Zhu, Y.; Xia, Y. *Angew. Chem., Int. Ed.* **2011**, DOI: 10.1002/anie.201107061.

(9) Love, J. C.; Estroff, L. A.; Kriebel, J. K.; Nuzzo, R. G.; Whitesides, G. M. *Chem. Rev.* **2005**, *105*, 1103.

(10) See details in the Supporting Information.

(11) (a) Chen, H.; Abraham, S.; Mendenhall, J.; Delamarre, S. C.; Smith, K.; Kim, I.; Batt, C. A. *ChemPhysChem* **2008**, *9*, 388. (b) Feng, Y. H.; Xing, S. X.; Xu, J.; Wang, H.; Lim, J. W.; Chen, H. *Dalton Trans.* **2010**, *39*, 349. (c) Chen, T.; Yang, M. X.; Wang, X. J.; Tan, L. H.; Chen, H. *J. Am. Chem. Soc.* **2008**, *130*, 11858.

(12) Feng, Y.; Wang, Y.; Wang, H.; Chen, T.; Tay, Y. Y.; Yao, L.; Yan, Q.; Li, S.; Chen, H. *Small* **2011**, DOI: 10.1002/smll.201102215.